Langmuir
Article
pubs.acs.org/Langmuir

Interfacing Neurons both Extracellularly and Intracellularly Using Carbon−Nanotube Probes with Long-Term Endurance

Shih-Rung Yeh,[†,#] Yung-Chan Chen,[‡,#] Huan-Chieh Su,[§,#] Tri-Rung Yew,[§,#] Hsiu-Hua Kao,[†] Yu-Tao Lee,[⊥] Tai-An Liu,[†] Hsieh Chen,[§] Yen-Chung Chang,[†] Pin Chang,[∥] and Hsin Chen*[,‡]

[†]*Institute of Molecular Medicine, National Tsing Hua University (NTHU), 101, Sec. 2, Kuang-Fu Rd., Hsinchu, Taiwan 300,* [‡]*Institute of Electronics Engineering, NTHU, Hsinchu, Taiwan 30013,* [§]*Department of Materials Science and Engineering, NTHU, Hsinchu, Taiwan 30013,* [⊥]*Institute of Nano Engineering and Micro System, NTHU, Hsinchu, Taiwan 30013, and* [∥]*Microsystem Technology Center, ITRI, Tainan, Taiwan 709*
[#] *These authors contributed equally to this work*

Received January 21, 2009. Revised Manuscript Received March 27, 2009

This study demonstrates that carbon nanotubes (CNTs) can be fabricated into probes directly, with which neural activity can be monitored and elicited not only extracellularly but also intracellularly. Two types of CNT probes have been made and examined with the escape neural circuit of crayfish, *Procambarus clarkia*. The CNT probes are demonstrated to have comparable performance to conventional Ag/AgCl (silver/silver cloride) electrodes. Impedance measurement and cyclic voltammetry further indicate that the CNT probes transmit electrical signals through not only capacitive coupling but also resistive conduction. The resistive conduction facilitates the recording of postsynaptic potentials and equilibrium membrane potentials intracellularly as well as the delivery of direct-current stimulation. Furthermore, delivering current stimuli for a long term is found to enhance rather than to degrade the recording capability of the CNT probes. The mechanism of this fruitful result is carefully investigated and discussed. Therefore, our findings here support the suggestion that CNTs are suitable for making biocompatible, durable neural probes of various configurations for diverse applications.

1. Introduction

Neurons employ potential differences across their membranes to transmit signals within themselves and among each other. This particular way of communication allows neural activity to be monitored and elicited with an electrode either *extracellularly* or *intracellularly*. In the extracellular approach, electrodes are placed intimately beside a neuron to record or to stimulate its electrical activity by capacitive coupling. The coupling efficiency depends very much on the impedance across the neural membrane, the electrode impedance, and the proximity to the neuron. With limited coupling efficiency, extracellular recording is adequate to detect action potentials of a neuron but not small postsynaptic potentials occurring during neuronal interactions. As monitoring PSPs is very important for studies like neural plasticity, a sharp glass pipet with an Ag/AgCl electrode inside has been employed to penetrate a neuronal membrane and thus to measure the potential of the intracellular fluid. The intracellular approach allows action potentials and postsynaptic potentials to be measured with better selectivity and signal-to-noise ratio. In addition, the reduction−oxidation (abbreviated as "redox" in the following) process between Ag and AgCl allows direct currents to be transmitted through the Ag/AgCl−electrolyte interface. This characteristic is particularly crucial to enable the recording of equilibrium membrane potential and the delivery of direct-current stimuli. However, the AgCl coating normally reduces into Ag completely after several hours of usage, impeding the two crucial functions.

In order to investigate the functional behavior of the brain as well as to develop neural prostheses, a variety of technologies and materials has been further proposed for interfacing a large number of neurons in parallel.[1−6] The common feature of all technologies is exploiting microfabrication to enhance the spatial resolution of neural recording and stimulation. However, significant reduction in electrode size increases electrode impedance greatly, limiting the recording sensitivity and the maximum stimulating current deliverable through an electrode.[7] Under these concerns, the carbon nanotube (CNT) with intriguing physicochemical property[8−13] has become an attractive material for the neuro-electronic interface.[14−20] By growing CNTs on microelectrodes,[14,15,19,20] the nanostructure of CNTs inherently

*Corresponding author: e-mail hchen@ee.nthu.edu.tw; Fax +886-35162221.

(1) Rutten, W. L. C. *Annu. Rev. Biomed. Eng.* **2002**, *4*, 407–452.
(2) Patolsky, F.; Timko, B. P.; Yu, G.; Fang, Y.; Greytak, A. B.; Zheng, G.; Lieber, C. M. *Science* **2006**, *313*, 1100–1104.
(3) Hochberg, L. R.; Serruya, M. D.; Friehs, G. M.; Mukand, J. A.; Saleh, M.; Caplan, A. H.; Branner, A.; Chen, D.; Penn, R. D.; Donoghue, J. P. *Nature (London)* **2006**, *442*, 164–171.
(4) Lebedev, M. A.; Nicolelis, M. A. L. *Trends Neurosci.* **2006**, *29*, 536–546.
(5) Engel, A. K.; Moll, C. K. E.; Fried, I.; Ojemann, G. A. *Nat. Rev. Neurosci.* **2005**, *6*, 35–47.
(6) Merabet, L. B.; Rizzo, J. F.; Amedi, A.; Somers, D. C.; Pascual-Leone, A. *Nat. Rev. Neurosci.* **2005**, *6*, 71–77.
(7) He, B. *Neuron Engineering*; Kluwer Academic: Norwell, MA, 2005.
(8) Musameh, M.; Lawrence, N. S.; Wang, J. *Electrochem. Commun.* **2005**, *7*, 14–18.
(9) Shanmugam, S.; Gedanken, A. *Electrochem. Commun.* **2006**, *8*, 1099–1105.
(10) Gooding, J. J. *Electrochim. Acta* **2005**, *50*, 3049–3060.
(11) Yeh, M.-K.; Tai, N.-H.; Liu, J.-H. *Carbon* **2006**, *44*, 1–9.
(12) Banks, C. E.; Davies, T. J.; Wildgoose, G. G.; Compton, R. G. *Chem. Commun.* **2005**, 829–841.
(13) Moore, R. R.; Banks, C. E.; Compton, R. G. *Anal. Chem.* **2004**, *76*, 2677–2682.
(14) Gabay, T.; Ben-David, M.; Kalifa, I.; Sorkin, R.; Abrams, Z. R.; Ben-Jacob, E.; Hanein, Y. *Nanotechnology* **2007**, *18*, 035201.
(15) Nguyen-Vu, T. D. B.; Chen, H.; Cassell, A. M.; Andrews, R.; Meyyappan, M.; Li, J. *Small* **2006**, *2*, 89–94.
(16) Gheith, M. K.; Pappas, T. C.; Liopo, A. V.; Sinani, V. A.; Shim, B. S.; Motamedi, M.; Wicksted, J. P.; Kotov, N. A. *Adv. Mater.* **2006**, *18*, 2975–2979.
(17) Lovat, V.; Pantarotto, D.; Lagostena, L.; Cacciari, B.; Grandolfo, M.; Righi, M.; Spalluto, G.; Prato, M.; Ballerini, L. *Nano Lett.* **2005**, *5*, 1107–1110.
(18) Mazzatenta, A.; Giugliano, M.; Campidelli, S.; Gambazzi, L.; Businaro, L.; Markram, H.; Prato, M.; Ballerini, L. *J. Neurosci.* **2007**, *27*, 6931–6936.
(19) Wang, K.; Fishman, H. A.; Dai, H.; Harris, J. S. *Nano Lett.* **2006**, *6*, 2043–2048.
(20) Keefer, E. W.; Botterman, B. R.; Romero, M. I.; Rossi, A. F.; Gross, G. W. *Nat. Nanotechnol.* **2008**, *3*, 434–439.

increases the effective interfacial area between microelectrodes and neurons. CNTs have also been demonstrated as a biocompatible substrate that promotes neuronal growth, boosts neural activity,[17] and transmits electrical stimulation effectively.[16,18,20] These promising results lead to the attempt of fabricating CNTs into microelectrodes[19] or even nanoporbes[21] directly for neural recording and stimulation.

However, the mechanisms underlying the electrical coupling at the CNT−electrolyte interface remain not well-understood. Most studies indicated that CNT electrodes were like metal electrodes, relying on capacitive coupling to record and to stimulate neural activity.[14−16,19] Pretreatments to enhance the characteristic capacitance of CNT electrodes and to avoid electrode reactions have also been proposed.[19] On the other hand, the study by Mazzatenta et al.[18] showed that voltage pulses applied to extracellular CNT substrates were able to induce intracellular, direct-current responses similar to those induced by intracellular voltage stimuli. As this phenomenon could not be induced by capacitive coupling, this experiment has led to the debate on the intriguing mechanical coupling between CNTs and a neuronal membrane.[18,20]

In this study, two types of CNT probes have been made to "probe" neural activity not only extracellularly but also intracellularly. Unlike other CNT-coated microelectrodes,[14,15,19] the probes had only CNTs at the probe tips involved in interfacing neurons, facilitating the characterization of the CNT−electrolyte interface. With the well-characterized escape neural circuit of the crayfish, *Procambarus clarkia*,[22−24] the performance of the CNT probes was compared with that of conventional Ag/AgCl electrodes. As the electrophysiological experiment indicated that the CNT−electrolyte interface could also transmit direct-current signals, the CNT−electrolyte interface was further characterized by impedance measurement, cyclic voltammetry, and high-resolution imaging. The endurance of CNT probes for delivering direct-current stimuli was also examined. Based on these experimental results, the characteristics of the CNT−electrolyte interface and the challenge of developing nanoscale neural probes are discussed.

2. Materials and Methods

2.1. Carbon Nanotube (CNT) Probes. Multiwalled carbon nanotubes were synthesized by floating-catalyst chemical vapor deposition (CVD) at about 1100 °C and 700 mbar.[11] Benzene, ferrocene, thiophene, and hydrogen were used as the precursor, catalyst, promoter, and carrier gas, respectively. With van der Waals forces, the synthesized CNTs attracted each other to form a mass. A tweezer was then used to take out a bundle of multiwalled CNTs from the mass. The CNT bundles having a size of about 0.1−0.5 mm in diameter and 2 cm in length were used to fabricate the i (insulated)-CNT probe and the g (glass)-CNT probe shown in Figure 1a.

Both the i-CNT and the g-CNT probes were made by connecting one end of a CNT bundle to an Ag wire with silver glue. It is notable that there is no Ag wire beyond the connecting point; i.e., the CNT bundle in Figure 1a contains purely CNTs, instead of being Ag wire coated with CNTs. The i-CNT probe (Figure 1a$_1$) was then made by coating the surface except for the tip of the CNT bundle with insulating epoxy (No. 2258, Life Co. Ltd.). The g-CNT probe was instead made by placing the CNT bundle in a sharp glass pipet (Figure 1a$_2$). One end of the CNT bundle, around 3 mm long, was immersed in the 3 M KCl solution in the pipet tip, through which the g-CNT probe was able to interface neurons either extracellularly or intracellularly. For the intracellular interface, only the glass tip of the g-CNT probe penetrated the neuronal membrane, allowing the saline in the probe tip to be in contact with the intracellular fluid. The CNT bundle immersed in the saline was subsequently able to measure the intracellular potential or to inject currents into the intracellular fluid through the saline. On the other hand, the i-CNT probe was able to facilitate an extracellular interface as CNT-coated microelectrodes.[14,15,19,20] While most CNT-coated microelectrodes could not avoid materials (e.g., Ag or TiN) underneath the CNT coating from involving in the electrode−electrolyte interface, the configuration of both CNT probes ensured that only CNTs at the probe tips (about 0.15 mm in diameter) involved in neural recording and stimulation, guaranteeing interfacial characteristics dependent merely on the CNTs. Finally, an Ag/AgCl wire was immersed in the 3 M KCl solution in a glass pipet to form a conventional neural probe for comparison (Figure 1a$_3$).

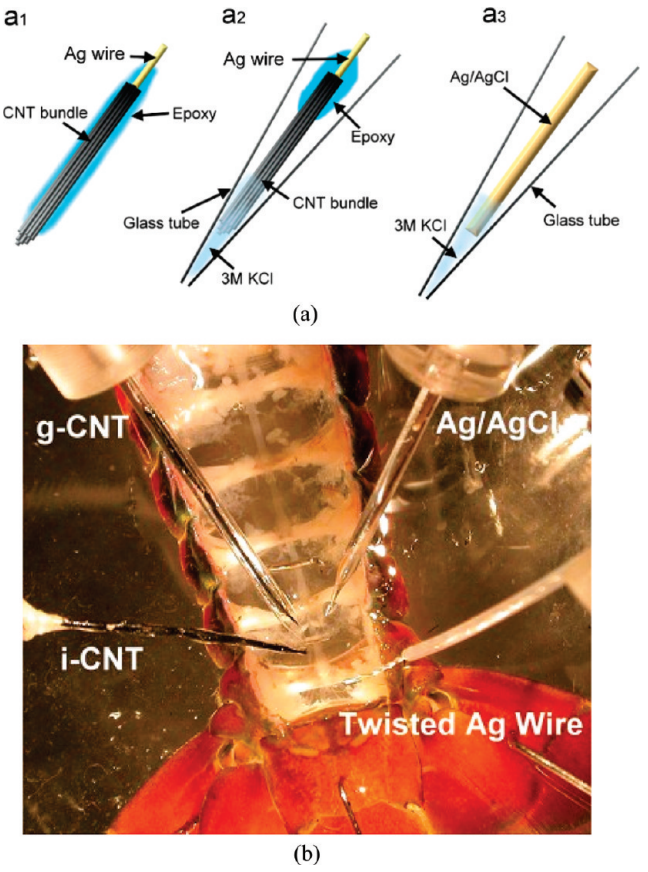

Figure 1. Diagrams of (a$_1$) the i (insulated)-CNT probe, (a$_2$) the g (glass)-CNT probe, and (a$_3$) the conventional Ag/AgCl glass pipet. (b) Experimental setup for characterizing the performance of the CNT probes with the escape neural circuit of the crayfish.

2.2. Neural Electrophysiological Experiments. Figure 1b shows the experimental setup for comparing the CNT probes with the conventional Ag/AgCl glass pipet. The abdomen of a crayfish was cut from the thorax, and the dorsal exoskeletons were removed. The preparation was then pinned on Sylgard in a 4.5 cm diameter Petri dish containing the crayfish saline (210 mM NaCl; 15 mM $CaCl_2$, 5.4 mM KCl, 2.6 mM $MgCl_2$, and 5 mM HEPES, pH 7.4). Both CNT probes and the Ag/AgCl glass pipet were in contact with lateral-giant (LG) neurons in the same (last) abdominal ganglion, which received inputs from the

(21) Kawano, T.; Cho, C. Y.; Lin, L. *Proc. 2nd IEEE Int. Conf. NEMS* **2007**, 895–898.
(22) Furshpan, E.; Potter, D. *J. Physiol.* **1959**, *145*, 289–329.
(23) Watanabe, A.; Grundfest, H. *J. Gen. Physiol.* **1961**, *45*, 267–308.
(24) Tsai, L.-Y.; Tseng, S.-H.; Yeh, S.-R. *J. Comp. Physiol., A* **2005**, *191*, 347–354.

mechanosensory afferents in the tail fin. A twisted, Teflon-coated silver wire was then employed to stimulate afferent neurons with voltage pulses to evoke compound EPSPs in the LG neuron. Once the afferent neurons were stimulated simultaneously by a higher voltage pulse, the amplitude of compound EPSPs exceeded the firing threshold, leading the LG neurons to generate an action potential and propagate the action potential into LG neurons in posterior ganglia. In this study, each measurement was repeated with four probes of the same type (n = 4). The recorded signals were digitalized at 100 kHz through a PCI-1602 A/D interface (ICP DAS, Taiwan), and subsequently, the digital data were stored and analyzed in a computer with a graphical user interface designed by the National Tsing Hua University, Taiwan.

2.3. Endurance Test. Conventional Ag/AgCl electrodes normally become unable to record neural signals faithfully as AgCl reduces into Ag completely. The degradation occurs easily especially when an Ag/AgCl electrode is used to deliver direct-current stimuli. Therefore, the CNT probes' endurance for physiological experiments was examined by forcing a pair of i-CNT probes to conduct a direct current in the 3 M KCl solution for a long period of time. The direct current was set precisely by connecting a source meter (Keitheley 2602) with the i-CNT probes in a closed loop. As the i-CNT probes had only CNTs at the cross section of the probe tip in contact with solutions, a nearly constant contact area between CNTs and the electrolyte was guaranteed regardless of the immersion depth of the probes. In addition, to make sure the impedance change due to CNTs' hydrophilicity[19] was negligible, all i-CNT probes were immersed in the 3 M KCl solutions for more than 20 h before the endurance test. The impedance spectra of the CNT−electrolyte interface before and after the current stress were then measured (Supporting Information) and compared, and so was the cyclic voltammetry[25] carried out. The scan rate of the cyclic voltammetry was 100 mV/s.

To investigate the impact of the current stress on the recording capability of i-CNT probes, a sinusoidal wave was transmitted into the 3 M KCl solution through an Ag/AgCl coil. The signals recorded by the i-CNT probe before and after the current stress were then compared. Finally, the change in recording capability was verified with the escape neural circuit of the crayfish. As the coupling efficiency of extracellular recordings depended very much on the proximity to neurons, the distance between the i-CNT probe and neurons had been carefully controlled between different recordings by using a mirco-manipulator (World Precision Instrument M3301) to handle the i-CNT probe.

3. Results

3.1. Neural Recording and Stimulation with CNT Probes. With the probe tip pressed against the LG axon, the i-CNT probe was able to detect an action potential of the LG neuron (indicated by an arrow in Figure 2a$_1$), as well as some small spikes associated with other LG neurons in the nerve cord (indicated by asterisks), evoked by an electrical shock on the sensory afferents via a twisted silver wire. The signal amplitude was 1.03 ± 0.35 mV, comparable to that detected by the Ag/AgCl glass pipet sucking on the same axon (0.89 ± 0.57 mV, Figure 2c$_1$). Conversely, as the i-CNT probe served as a stimulator to excite afferent neurons and the Ag/AgCl glass pipet recorded the LG neuron intracellularly, a single voltage pulse applied to the i-CNT probe was sufficient for exciting the afferent neurons and evoking compound EPSPs in the LG neuron. With a higher stimulating voltage, the amplitude of EPSPs exceeded the firing threshold and an action potential appeared (Figures 2a$_2$ and 2a$_3$ in the rectangular box). For the g-CNT probe, with the bevelled tip placed

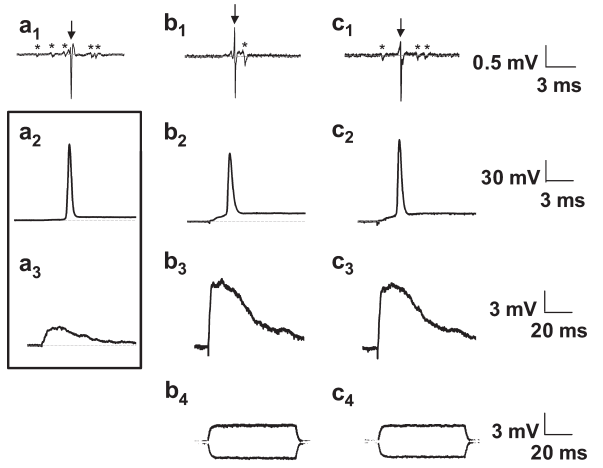

Figure 2. Stimulation and recording of lateral-giant neurons in crayfish via an i-CNT probe, a g-CNT probe, and an Ag/AgCl glass microelectrode. From the top to the bottom, the figure shows sequentially the respective extracellular recordings (a$_1$, b$_1$, c$_1$) of action potentials (the arrows indicate the spike of the LG neuron in contact with the probes, and the asterisks indicate the spikes of other neurons in the nerve cord.) elicited by stimulating afferent neurons via a bipolar electrode, intracellular recordings of an action potential (AP) and an excitatory postsynaptic potential (EPSP) induced by the extracellular stimulation via the i-CNT probe (a$_2$ and a$_3$ in the rectangle), intracellular recordings of APs and EPSPs with the g-CNT probe (b$_2$, b$_3$), intracellular recordings of APs and EPSPs with the Ag/AgCl microelectrode (c$_2$, c$_3$), the recordings of equilibrium membrane potentials by the g-CNT probe (b$_4$) in response to current injections through the Ag/AgCl electrode, and the recordings of equilibrium membrane potentials by the Ag/AgCl electrode in response to current injections through the g-CNT probe (c$_4$). Each measurement was repeated with four probes of the same type.

intimately to a LG neuron, the g-CNT probe was able to detect an action potential extracellularly with a magnitude of 0.89 ± 0.60 mV (indicated by the arrow in Figure 2b$_1$) and some small spikes (indicated by asterisks) evoked by an electrical shock on the sensory afferents. Moreover, a sharp g-CNT probe (with a tip resistance of 14.5 ± 2.4 MΩ) was used to impale the LG neuron. The penetration of the neuronal membrane was indicated by a sudden drop of the dc potential recorded by the g-CNT probe. After the penetration, the g-CNT probe was able to record the action potential intracellularly with a magnitude of 85.2 ± 5.84 mV (Figure 2b$_2$), comparable to that recorded by the Ag/AgCl glass pipet impaling the same neuron (88.4 ± 9.78 mV, Figure 2c$_2$). As the electrical shock on afferent neurons only induced compound EPSPs in the LG neuron, the g-CNT probe was still able to record the compound EPSP intracellularly with an magnitude of 5.14 ± 0.92 mV (Figure 2b$_3$), comparable to that recorded simultaneously by the Ag/AgCl electrode (4.67 ± 0.86 mV, Figure 2c$_3$). The g-CNT probe's ability to interface neuron intracellularly was thus clearly demonstrated. More interestingly, the g-CNT probe was found capable of recording equilibrium membrane potentials and delivering direct currents. As direct-current stimuli of ±10 nA was delivered into the Ag/AgCl glass pipet impaling an LG neuron, the g-CNT probe impaling the same neuron was able to detect the resulted equilibrium membrane potential intracellularly (1.58 ± 0.63 and −1.63 ± 0.38 mV, respectively, in Figure 2b$_4$). Conversely, as the direct-current stimuli of ±10 nA was delivered into the g-CNT probe, the Ag/AgCl glass pipet detected comparable changes in the membrane potential (1.57 ± 0.50 and −1.60 ± 0.4 mV,

(25) Mabbott, G. A. *J. Chem. Educ.* **1983**, *60*, 697–702.

respectively, in Figure 2c$_4$), indicating the stimuli were delivered effectively. This intriguing result suggested that the CNT−electrolyte interface exhibited resistive conduction to facilitate the transmission of direct currents and equilibrium potentials.

3.2. Endurance of the CNT Probe. With the setup shown at the top-right corner of Figure 3a, a pair of i-CNT probes was forced to conduct a direct current of 500 nA for 2 h. Let the electrochemical impedance of the CNT−electrolyte interface (Z_e) be modeled as a resistor (R) and a capacitor (C) in parallel, analogous to the constant-phase element described earlier.[15,26,27] The analytic equation of Z_e is given as

$$Z_e = Z_R // Z_C = \frac{R}{1 + (wRC)^2}(1 - jwRC) \quad (1)$$

where w denotes the radian frequency. Parts a and b of Figure 3 show the capacitive impedance ($|Z_C| = 1/wC$) and the resistive impedance ($Z_R = R$), respectively, measured before and after the current stress. Z_C was comparable to Z_R over the frequency bandwidth of neuronal signals (100−10 kHz), indicating that the CNT probes transmitted signals through both capacitive coupling and resistive conduction. This agreed with the phenomenon observed in the physiological experiment above. More interestingly, both Z_C and Z_R were reduced after the current stress, no matter the CNT probe was the anode or the cathode electrode in the endurance test. Similar reduction was also observed as the i-CNT probes were immersed in deionized water, implying that K^+ and Cl^- ions in 3 M KCl solution were not involved in the change of impedance. This intriguing result leads to several questions. First, what reactions supported the resistive conduction? Second, what mechanisms caused the impedance change? Third, would the impedance continue to improve with the duration of the current stress? These questions were investigated by comparing with purified CNTs and elongating the current-stress process.

3.3. Comparison with Purified CNTs. The resistive conduction at the CNT−electrolyte interface could relate to amorphous carbon impurities, catalyst particles, and abundant functional groups such as edge-plane defects and oxygenated species on the CNT surface.[8−10,28] To reduce amorphous carbon impurities and catalyst particles, the as-grown CNTs were purified by the following steps. (1) The pristine CNTs were heated in a microwave with a power of 200 W for 5 min. (2) The CNTs were then washed with concentrated HCl acid by sonication for 15 min. (3) The CNTs were further rinsed with methanol and DI water and then dried. The steps were repeated twice to remove impurities as much as possible. The curves with circular symbols in Figure 3 show the impedance of the purified CNTs for comparison with that of the as-grown CNTs (rectangular symbols) and the stressed CNTs (triangular symbols). Obviously, the purification process also led to the reduction in impedance. If the resistive conduction were dominated by the reactions with impurities, the purification process would have led to increase in resistive impedance. Therefore, the resistive conduction was more likely to be dominated by reactions with abundant functional groups or edge-plane defects. Figure 4 shows the scanning electron microscopy (SEM) images of the as-grown CNTs, the

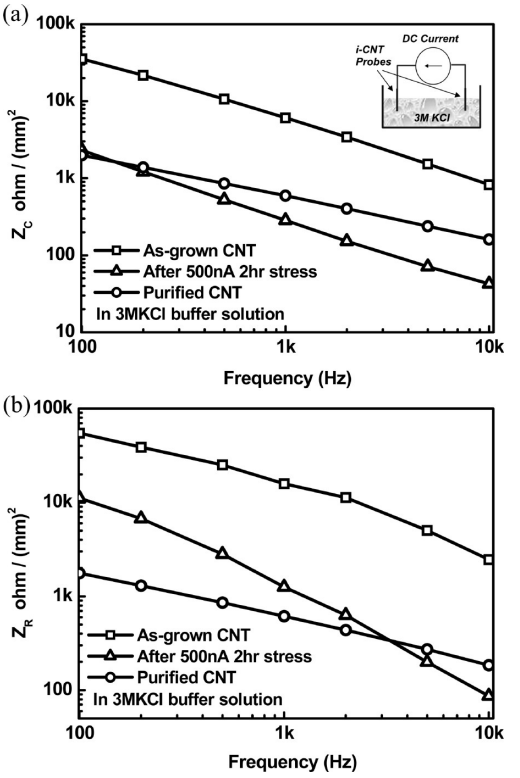

Figure 3. (a) Capacitive and (b) resistive impedance of the i-CNT probe measured before (black curves) and after (blue curves) the current-stress process. The capacitive and resistive impedance of the same CNTs undergoing the purification process is also shown (red curves).

stressed CNTs, and the purified CNTs. Both the stressed CNTs and the purified CNTs had less impurity particles than the as-grown CNTs. The reduction of impurities after the current stress was especially obviated by the diminished images at the bottom-right corners of Figure 4a,b. This indicated that the current-stress process had analogous effects to the purification process, agreeing with the impedance spectra shown in Figure 3.

3.4. Stress-Induced Impedance Reduction. To investigate the cause of impedance reduction after the current stress, the current-stress process was elongated and repeated. As the hydrophilicity of CNTs was of concern, the i-CNT probes were first immersed in the 3 M KCl solution for 24 h, left dried in the air at room temperature for 8 h, and immersed in the solution for 24 h again. The CNT probes were then stressed with the same condition (500 nA for 2 h) in section 3.2 for four cycles. Afterward, the CNT probes were kept in the 3 M KCl solution for 12 h and then stressed for another two cycles. Finally, the CNT probes were kept in the 3 M KCl solution for 90 h. The CNT probes were immersed in the same solution all the time since the first stressing cycle, in order to avoid impedance changes due to the dehydration of the CNTs. The cyclic voltammetry was carried out at each stage of the current-stress process, and the characteristic capacitance of the CNT−electrolyte interface was derived from the cyclic voltammograms. Let C_I represent the characteristic capacitance of the CNT−electrolyte interface, relating to the Z_C in section 3.2 as $Z_C = 1/wC_I$. C_I was derived according to

$$\Delta i = 2C_I \frac{dV}{dt} \quad (2)$$

where Δi is the maximum current difference between the positive and the negative voltage sweeps.[15]

(26) Li, J.; Koehne, J. E.; Cassell, A. M.; Chen, H.; Ng, H. T.; Ye, Q.; Fan, W.; Han, J.; Meyyappan, M. *Electroanalysis* **2005**, *17*, 15–27.
(27) Yang, S.; Huo, J.; Song, H.; Chen, X. *Electrochim. Acta* **2008**, *53*, 2238–2244.
(28) Nugent, J. M.; Santhanam, K. S. V.; Rubio, A.; Ajayan, P. M. *Nano Lett.* **2001**, *1*, 87–91.
(29) Vazquez, E.; Georgakilas, V.; Prato, M. *Chem. Commun.* **2002**, 2308–2309.

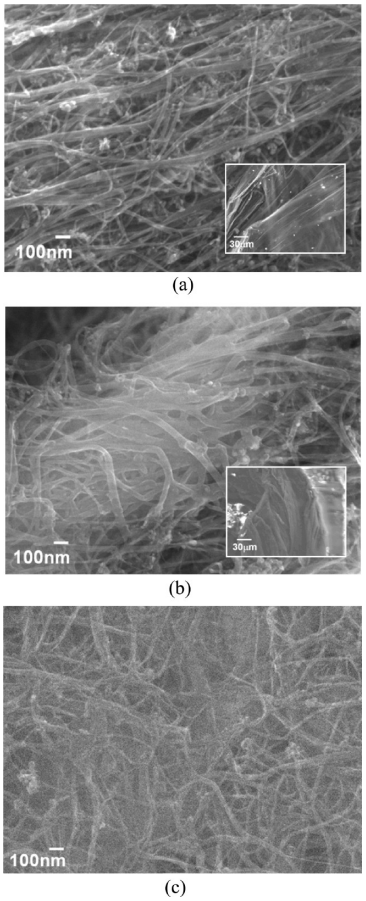

Figure 4. SEM images of (a) the as-grown CNTs, (b) the current-stressed CNTs, and (c) the purified CNTs. The insets at the bottom-right corners of (a) and (b) give the images diminished by 100 times.

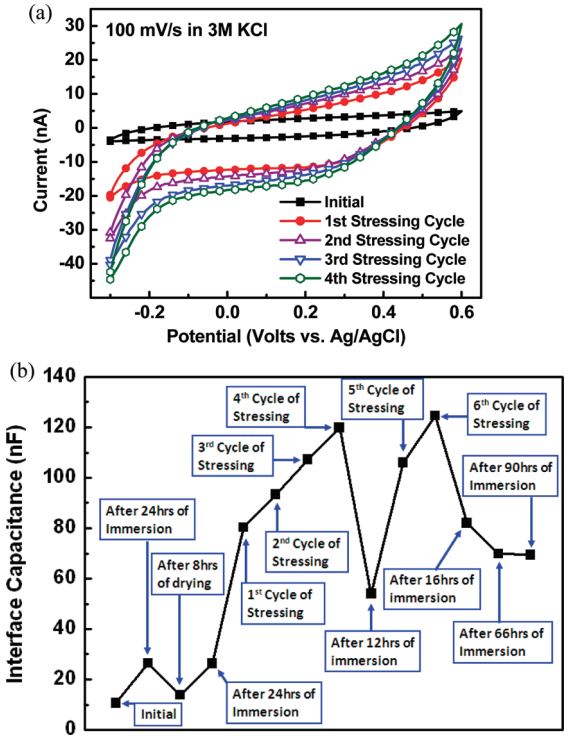

Figure 5. (a) Cyclic voltammograms of the i-CNT probe measured at different stages of an elongated current-stress process. In each stressing cycle, the i-CNT probes were forced to conduct a dc current of 500 nA for 2 h. (b) Corresponding change in characteristic capacitance during the current-stress process (at a scan rate of 100 mV/s).

Figure 5a shows the cyclic voltammograms in the first four stressing cycles. Δi increased with the number of stressing cycles, so did C_I. The increment in the first cycle was significantly larger than those in the following three cycles. The increment was thus likely to saturate into a maximum value as the current stress was prolonged. Nevertheless, C_I had increased by 6 times after four stressing cycles, comparable to the improvement introduced by the acid pretreatments proposed by Hu et al.[30]

Figure 5b further shows the change of C_I through the entire experiment. The first four data points revealed that C_I changed with the extent of the hydration of CNTs. Long-term immersion allowed the electrolyte to diffuse into the CNT bundles, increasing the interfacial area with CNTs and thus C_I. However, the "wet-induced" impedance change was slow and was completely gone after the dehydration of CNTs. On the contrary, the current stress caused C_I to increase more rapidly and significantly (the first−fourth cycles in Figure 5b). Although the "stress-induced" increase in C_I was lost by more than a half after 12 h of the static immersion, C_I did not reduce to the original value measured before the current stress. Resuming the current stress caused C_I to increase significantly again (the fifth and sixth cycles in Figure 5b), while the following immersion caused C_I to decrease again, but not to the value measured before the fifth stressing cycle. Finally, C_I saturated to a constant value after 66 h immersion in the solution. This interesting phenomenon indicated that the stress-induced impedance change contained both permanent and nonpermanent components. The underlying mechanisms will be discussed carefully in section 4.3.

3.5. Electrically Enhanced Recording Capability. To demonstrate how the impedance change affected the recording capability, an i-CNT probe was used to record a 12 mV_{pp}, 50 Hz sinusoidal signal in the 3 M KCl solution. Figure 6a shows the signals recorded by the i-CNT probe before and after the current stress of 5 μA for 4 h. Obviously, the signal recorded by the stressed i-CNT probe exhibited greater amplitude and less phase error, indicating that the impedance reduction (both Z_R and Z_C) improved the recording capability. According to eq 1, the increase in amplitude was attributed to the reduction in $|Z_e|$, i.e., the reduction in both Z_R and $|Z_C|$, as obviated by Figure 3. On the other hand, the reduced phase error was attributed to the reduction in $wRC = Z_R/|Z_C|$.

The improvement was further verified with the escape neural circuit of the crayfish. As shown in Figure 6b, the action potential recorded by the stressed i-CNT probe exhibited a slightly larger amplitude. This result confirmed that the current stress increased the characteristic capacitance (i.e., reduced Z_C), since extracellular recording mainly relied on capacitive coupling. Moreover, the timing difference between the action potentials in the two recordings should be attributed to the change in the excitability of the LG neurons between different experimental trials. Depending on the position of the stimulating electrodes, the population of sensory afferent neurons being excited could also differ from one trial to another, resulting in different time delay for evoking an action potential in the LG neuron. Finally, it is notable that the effect of the reduction in Z_R on neural recording is difficult to demonstrate. While Z_R mainly affects the recording of low-frequency signals, Z_R is much smaller than the tip resistance of the glass pipet (e.g., g-CNT probes had tip resistance of

(30) Hu, C.-C.; Su, J.-H.; Wen, T.-C. *J. Phys. Chem. Solids* **2007**, *68*, 2353–2362.

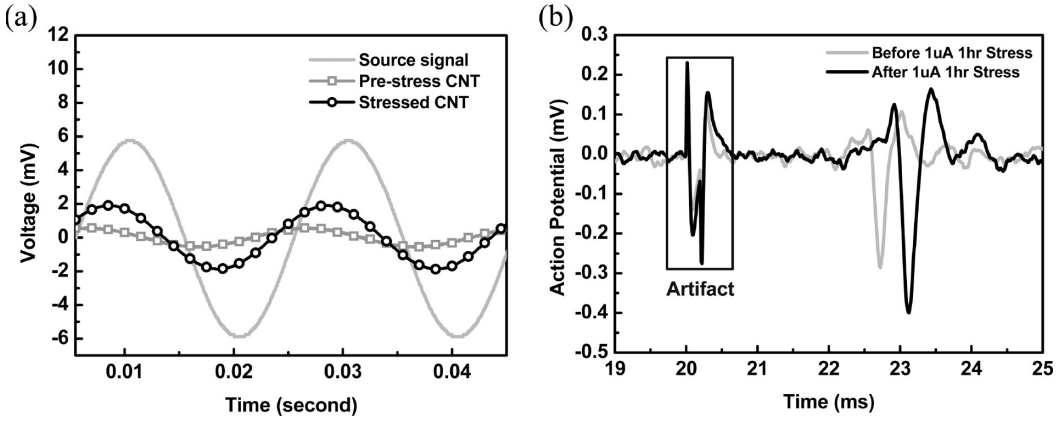

Figure 6. (a) Source signal (black) in the 3 M KCl solution and the corresponding signals recorded by an i-CNT probe before (green) and after (orange) the current stress. (b) Action potentials of lateral-giant neurons recorded by an i-CNT probe before and after the current stress.

14.5 ± 2.4 MΩ), making it difficult to observe the effects of Z_R on intracellular recording.

4. Discussion

4.1. Capability of the CNT Probes. This study demonstrates that the CNT probes are capable of recording and stimulating neural activity not only extracellularly but also intracellularly. While the results of extracellular experiments agree with those demonstrated with CNT-coated microelectrodes,[14,15,19] intracellular recording and stimulation with CNT probes are explored for the first time. More importantly, the impedance measurements indicate that the CNTs used in our experiments exhibit not only capacitive but also resistive characteristics, contrary to the suggestion that capacitive impedance dominates.[14,15,19] This resistive characteristic is especially crucial for the g-CNT probes to record equilibrium membrane potentials and to deliver direct-current stimuli as effectively as conventional Ag/AgCl electrodes. The intracellular, direct-current response induced by extracellular CNT substrates observed in Mazzatenta et al.[18] could also be partly attributed to the resistive characteristic.

4.2. Resistive Conduction of the CNT Probes. The comparison between the current-stressed and the purified CNTs suggested that the resistive conduction of the CNT probes should rely more on reactions with abundant functional groups on the CNT surface, such as edge plane defects and oxygenated species.[8−10,28] This suggestion is further supported by two other results. First, although reactions with catalyst impurities like Fe could contribute to the resistive conduction, the cyclic voltammograms measured at different scan rates show no significant redox process, i.e., current peaks, in the voltage range of neural recording (−0.1 to 0.1 V), as is also reported earlier.[15,19] Second, the typical high-resolution transmission electron microscopy (HRTEM) images of the CNT bundles (Supporting Information) indicate that both the as-grown and the current-stressed CNTs do not exhibit many amorphous carbon impurities. The resistive conduction of the CNT probes, especially for the stressed ones, is thus less likely to be dominated by reactions with amorphous carbon and catalyst impurities. Compared to the more conventional carbon fiber electrodes, the CNT probes are more analogous to the CNT electrodes used in Nugent et al.'s experiment,[28] whose structure and topology are very different from that of graphite fibers, and are shown to favor fast electron-transfer kinetics (i.e., resistive conduction).

4.3. Electrically Induced Impedance Change. In the endurance test, the impedance of the CNT probes decreases rather than increases after conducting direct currents for a long time. Therefore, unlike other metal electrodes (e.g., Pt) or the Ag/AgCl electrodes,[1,7] long-term usage improves rather than degrades the recording capability of the CNT probes. Although the impedance improvement can largely diminish if CNT probes are kept "quiet" (not in use), the impedance always reduces to favor neural recording and stimulation during usage. This intriguing characteristic makes CNTs particularly attractive for interfacing neurons. The impedance improves by more than 3 times after a current stress for just 2 h (Figure 4b), and the cyclic voltammograms (Figure 4a) display no significant redox processes after the current stress, eliminating the concern over the formation of new compounds or the release of toxic chemicals. Compared to the acid pretreatments proposed in Hu et al.,[30] H_2SO_4 or HNO_3 employed in the acid pretreatments could be toxic for neurons if the acids were not rinsed completely. Under this concern, enhancing impedance by the current stress is more favorable.

An elongated current-stress process further suggests that the impedance improvement could result from several mechanisms. The first was the "polishing" effect on the CNT surface. During the current stress, the voltage across the CNT probes (around 1.3 V) was greater than the hydrolysis voltage, causing hydrolysis reactions to remove particles absorbed on the CNT surface (Figure 4). The interfacial area between the CNTs and the electrolyte thus increased and resulted in smaller impedance. Second, the optical microscope images (Supporting Information) further indicated that the current stress also caused CNTs to disperse slightly more in the electrolyte. The dispersion of CNTs also led to the increase in the interfacial area and thus the reduction in impedance. Third, the current stress could cause the pH value around the CNT surface to vary during the hydrolysis reaction, inducing more edge-plane defects or functional groups on the CNT surface as the acid or oxidation treatments did.[19,30,31] The existence of this mechanism is supported by the emergence of a current peak around −0.2 V in Figure 5a after the current stress, and the current peak should correspond to the reduction of adsorbed oxygen.[30,31] The first two mechanisms are physical changes, while the third is chemical change. Therefore, the nonpermanent impedance change shown in Figure 5b could relate to the first two mechanisms, while the permanent impedance change to the third. For example, once the i-CNT probes were immersed in the buffer solution for a long time, particles could adhere to the CNT surface again or the

(31) Barisci, J. N.; Wallace, G. G.; Baughmann, R. H. *J. Electroanal. Chem.* **2000**, *488*, 92–98.

dispersion effect could diminish, leading the impedance to increase again.

4.4. Nanoscale Neural Probes. As the CNTs have been shown capable of probing neural activity intracellularly with promising endurance, it will be interesting to develop a nanoscale neural probe using only a single CNT as the probe tip.[21] Such a nanoscale probe will not only facilitate long-term, intracellular interface with neurons but also minimize the damage to neurons. Although extracellular CNTs could also couple intracellular signals noninvasively,[18] the mechanism remains under debate and the coupling efficiency could be not enough for recording miniature neural activity like PSPs. The nanoscale probe thus provides a good option. However, the impedance of a single CNT could be too large for practical neural recording and stimulation. According to Figure 3, the i-CNT probe with a diameter of 150 μm has an interfacial area of 17 671 μm^2 and a total impedance of 14 kΩ at 1 kHz. Given that the impedance is inversely proportional to the area, a single, multiwalled CNT with a diameter of 10 nm has a surface area of 0.03 μm^2 per micrometer in length. This corresponds to an estimated impedance of 8.25 GΩ at 1 kHz and 825 GΩ at 10 Hz, too large for neural recording and stimulation. As the input impedance of recording amplifiers can hardly exceed 100 GΩ,[32,33] at least 100 CNTs are required for reducing the impedance to a reasonable value (< 10 GΩ at 10 Hz). However, 100 CNTs piled up in the densest hexagonal structure have a diameter of about 100 nm, not much smaller than the diameter of conventional glass micropipets (200 nm). Therefore, technologies for growing a single CNT longer than 10 μm, as well as the use of single-walled CNT with a diameter of around 1 nm,[34] are crucial for releasing the constraint.

In addition, the CNT probes used in our experiments have not been purified to remove impurities such as metallic catalyst, which is normally toxic to neurons. Although the toxic impurities can be removed by the purification process proposed by Vazquez et al.,[29] for example, extra rinsing will be important to remove the toxic acids completely. In addition, the acid treatment and rinsing could detach CNTs from the substrate on which they are grown to form nanoscale probes. It is thus important to consider how to purify CNTs in the nanoscale probes. As the current stress has been shown to have analogous effects to the purification process, the current stress could be an optional approach while the effectiveness should be evaluated and compared to the standard purification process.

5. Conclusions

By fabricating two types of CNT probes and testing the probes with the well-characterized crayfish system, we have demonstrated that CNT probes can monitor and stimulate neural activity not only extracellularly but also intracellularly, with comparable performance to conventional Ag/AgCl glass pipettes. The promising performance in intracellular recording is first explored and proved to rely on CNTs' respectrable resistive characteristics. The impedance spectra and SEM images of the CNT probes and purified CNTs indicate that the resistive conduction rely mainly on the abundant functional groups on the CNTs. More interestingly, the impedance of the CNT−electrolyte interface is found to improve with the delivery of current stimuli, making CNT probes particularly suitable for long-term usage. This fruitful durability is likely to result from the polishing effects, water penetration, and the increase of functional groups induced by the hydrolysis reactions. The impedance improves comparably to that induced by acid pretreatments. As the CNT probes proposed in this research are not difficult to fabricate, the purified CNT probes will provide neuroscientists with an optional neurophysiological tool which is biocompatible, reliable, and durable. Moreover, technologies for growing long CNTs on microfabricated substrate will be developed to realize nanoscale neural probes of various configurations for diverse applications.

Acknowledgment. This work was supported by the National Science Council, Taiwan (Grant Code: 96-2627-E-007, 2007-2010).

Supporting Information Available: Measurement setup of electrochemical impedance spectroscopy, the HRTEM inages of the CNT bundles, and the optical microscopy images of the CNT bundles. This material is available free of charge via the Internet at http://pubs.acs.org.

(32) Harrison, R. R.; Charles, C. *IEEE J. Solid-State Circuits* **2003**, *38*, 958–965.
(33) Chandran, A. P.; Najafi, K.; Wise, K. D. *IEEE Proc. First Joint BMES/EMBS Conf.* **1999**, 386.
(34) Iijima, S.; Ichihashi, T. *Nature (London)* **1993**, *363*, 603–605.